The nonlinear Northern Hemisphere winter atmospheric response to ENSO

Aiming Wu and **William W. Hsieh**
Dept. of Earth and Ocean Sciences, University of British Columbia
Vancouver, B.C., Canada, V6T 1Z4
Tel: (604) 822-3932, Fax: (604) 822-6088
E-mail: awu@eos.ubc.ca

Geophys. Res. Lett. (revised)

December 25, 2003

Abstract

A nonlinear projection of the tropical Pacific sea surface temperature anomalies (SSTA) onto the Northern Hemisphere winter 500-mbar geopotential height (Z500) by a neural network reveals asymmetric atmospheric patterns associated with El Niño and La Niña. While the linear response of Z500 to tropical Pacific SSTA is largely confined over North Pacific and North America, the nonlinear response, mainly a quadratic response to the SSTA, reveals that regardless of the sign of the SSTA, positive Z500 anomalies are found over the central-eastern North America, North Atlantic and western Europe, and negative Z500 anomalies over the west coast of North America, Scandinavia and eastern Europe— consistent with the positive Pacific-North America (PNA) teleconnection pattern and the positive North Atlantic Oscillation (NAO) pattern being excited.

1 Introduction

The climate of the tropical Pacific is dominated by an irregular interannual fluctuation known as the El Niño-Southern Oscillation (ENSO), where a warm episode is called an El Niño, and a cold episode, a La Niña. The classical paradigm that the extratropical atmosphere responds linearly to opposite phases of ENSO via teleconnection [*Wallace and Gutzler*, 1981] has been questioned by recent evidence from climate statistics and numerical models, suggesting that the global atmospheric response to the tropical Pacific sea surface temperature (SST) anomalous forcing is inherently nonlinear [*Hoerling et al.*, 1997, 2001; *Sardeshmukh et al.*, 2000; *Hannachi*, 2001; *Wu et al.*, 2003]. The North America winter climate response to ENSO shows an eastward phase shift of the circulation anomalies (by about 35°) between the composites of warm ENSO episodes and the composites of cold episodes, with the two wave trains manifesting different tropical origins [*Hoerling et al.*, 1997]. Composites of observed surface air temperature and precipitation anomaly over North America during El Niño years are also not exactly anti-symmetrical to those during La Niña years [*Shabbar et al.*, 1997; *Montroy et al.*, 1998]. *Pozo-Vázquez et al.* [2001] mentioned that, in the North Atlantic area, no statistically significant sea level pressure (SLP) anomaly patterns were found associated with warm episodes, while during cold episodes a statistically significant SLP anomaly pattern resembling the positive phase of the North Atlantic Oscillation (NAO) [*Hurrell*, 1995] was found, suggesting a nonlinear association between the Euro-Atlantic climate and ENSO.

If x denotes an ENSO index, and if y is the extratropical atmospheric response to ENSO, how does one derive the nonlinear response function $y = f(x)$? A linear f is easily obtained by regressing the atmospheric variables upon an ENSO SST index, yielding atmospheric spatial patterns associated with the SSTA [e.g., *Deser and Blackmon*, 1995]. In this linear projection of the ENSO index to the atmospheric variables, the atmospheric patterns during El Niño are by definition strictly anti-symmetrical to those during La Niña. Composite analysis computes the atmospheric patterns by averaging the data over the years when warm episodes occurred, and averaging over cold episodes. While the patterns during warm and cold episodes are not forced to be anti-symmetrical, composite analysis does not yield a nonlinear response function. "One-sided linear regression", which calculates the linear regression between all occurrences of one sign of the SST index and the corresponding response variable [*Hoerling et al.*, 2001], fits to an $f(x)$ forced to be linear for $x > 0$ and for $x < 0$ — a very restrictive class of nonlinear functions. Nonlinear canonical correlation analysis (NLCCA), a newly developed technique using neural networks (NN) [*Hsieh*, 2001], has been applied to the observed SST and an ensemble of atmospheric general circulation model (AGCM) simulations [*Wu et al.*, 2003], where asymmetries occurred between El Niño and La Niña in the nonlinear mode for both the SST and atmospheric anomaly fields. The disadvantage of the NLCCA is that it trains three NNs separately and has a rather large number of model parameters, which requires many samples to obtain robust results when trying to extract weak signals. In short, extracting the general nonlinear response function of the atmosphere to ENSO has so far been elusive.

In the present work, a nonlinear projection of the ENSO SST index to the Northern Hemisphere winter (November to March) 500-mbar geopotential height (Z500), via a NN, is used to obtain the nonlinear response function $f(x)$, and the nonlinear Z500 anomaly patterns associated with ENSO. The SST index used is the leading principal component (PC) of the winter SSTA over the tropical Pacific.

2 Data and methodology

The monthly Z500 data from January 1950 to March 2003 with 2.5° by 2.5° resolution were obtained from the National Centers for Environmental Prediction (NCEP) reanalysis datasets at the NOAA-Cooperative Institute for Research in Environmental Sciences (NOAA-CIRES) Climate Diagnostic Center [*Kalnay et al.*, 1996]. Anomalies were calculated by subtracting the monthly climatology based on 1950-2002 period. Data over the Northern Hemisphere (20°N to the North Pole) and during the winter season (November–March) were used, thus the total number of months was 268. After removing the linear trend and weighing the anomalies by the square root of the cosine of the latitude, principal component analysis (PCA) was used to compress the data, with the 10 leading principal components (accounting for 76% of the variance) retained.

The SST index is the standardized first PC of the winter (November–March) SSTA over the tropical Pacific (122°E-72°W, 22°S-22°N with a resolution of 2°×2°). The monthly Extended Reconstructed Sea Surface Temperatures (ERSST) were downloaded from the National Climate Data Center (NCDC), National Oceanic and Atmospheric Administration (NOAA, ftp.ncdc.noaa.gov/pub/data/ersst). Anomalies were calculated by subtracting the monthly climatology, and linear trend removal was performed prior to PCA.

The multi-layer perceptron NN model with 1-hidden layer used here has a similar structure to the multivariate nonlinear regression model used for ENSO prediction by our group [*Hsieh and Tang*, 1998], except that it has only one predictor (the SST index) and multiple response variables (the 10 leading PCs of the Z500 anomalies). The input SST index is first nonlinearly mapped to four intermediate variables (called hidden neurons), which are then linearly mapped to 10 output variables. With enough hidden neurons, the NN is capable of modeling any nonlinear continuous function to arbitrary accuracy. Starting from random initial values, the NN model parameters are optimized so that the mean square error (MSE) between the 10 model outputs and the 10 leading PCs of the Z500 anomalies is minimized. To avoid local minima during optimization [*Hsieh and Tang*, 1998], the NN model was trained repeatedly 30 times from random initial conditions and the solution with the smallest MSE was chosen and the other 29 rejected.

To reduce the possible sampling dependence of a single NN solution, we repeated the above calculation 400 times with a bootstrap approach. A bootstrap sample was obtained by randomly selecting data (with replacement) 268 times from the original record of 268 months, so that on average about 63% of the original record was chosen in a bootstrap sample [*Efron and Tibshirani*, 1993]. The ensemble mean of the resulting 400 NN models was used as the final NN solution, found to be insensitive to the number of hidden neurons, which was varied from 1 to 5 in a sensitivity test.

3 Results

The climate signal extracted by the nonlinear projection is manifested by a curve in the 10-dimensional phase space of the Z500 PCs; in contrast, the linear projection extracts a straight line in the same 10-D space. This curve was parabola-like (not shown) when viewed in the PC_1-PC_2 plane and in the PC_1-PC_3 plane, indicating that the Z500 response to the SST index is a nonlinear combination of some of its leading PC modes. For a specific value of the SST index, the NN solution gives the 10 Z500 PCs, which when combined with the corresponding spatial patterns of the PCs (called the empirical orthogonal functions, EOFs), yields the Z500 spatial anomalies associated with the given SST. As the SST index varies, both the pattern and amplitude of the Z500 spatial anomalies change, in contrast to the linear projection method, which gives a fixed spatial pattern and a variable amplitude.

When the SST index takes on its minimum value (i.e. strong La Niña), three large anomalies appear in the Z500 anomaly field (Fig. 1a) over North Pacific and North America, resembling a negative Pacific–North America (PNA) teleconnection pattern [*Wallace and Gutzler*, 1981], with negative height anomalies over western Canada. We also see positive anomalies over the North Atlantic and western Europe, which are linked to the positive anomalies over eastern Canada and the United States (US), and negative anomalies over Scandinavia and eastern Europe, connected to the negative anomalies over western Canada via the North Pole. When the SST index takes on its maximum value (strong El Niño), the negative PNA pattern in Fig. 1a has turned into a positive PNA pattern (Fig. 1d), with anomaly centers shifted eastward by 30-40° and with magnitude approximately doubled over the

North Pacific and Canada. In both Figs. 1a and 1d, negative height anomalies are found over the west coast of North America, and positive anomalies over eastern Canada and northeastern US. Also, the anomalies over the Atlantic ocean and Europe are maintained in Fig. 1d, but with about a 15° eastward shift. Clearly, the Z500 anomalies associated with strong El Niño are not simply a mirror image of those associated with strong La Niña.

Figs. 1b and 1e show the anomalies associated with the half minimum and half maximum SST index respectively. The Z500 anomalies decrease in magnitude, especially over the North Atlantic and Europe areas. The anti-symmetry between Fig. 1b and 1e is much more conspicuous than that between Fig. 1a and 1d, consistent with the notion that appreciable SSTA are required for initiating a nonlinear atmospheric response [*Hoerling et al.*, 2001].

To reveal the nonlinear response in the Z500 anomalies to the tropical SSTA, we plotted in Fig. 1c the difference between the Z500 anomalies in Fig. 1a and double the anomalies in Fig. 1b; and similarly in Fig. 1f, the difference between the anomalies in Fig. 1d and double the anomalies in Fig. 1e. Interestingly, despite the large difference between Figs. 1a and 1d, and the smaller difference between Figs. 1b and 1e, the Z500 anomalies in Figs. 1c and 1f agree well with each other, indicating that regardless of the sign of the SST index, the nonlinear response has positive Z500 anomalies appearing over the central-eastern North America, North Atlantic and western Europe, and negative Z500 anomalies over the west coast of North America, Scandinavia and eastern Europe. The anomaly pattern in Fig. 1c or 1f is consistent with the positive phase of the PNA teleconnection and the positive phase of the NAO being excited.

Next PCA is used to analyze the field of Z500 anomalies resulting from our nonlinear projection of the SST index during Jan. 1950–Mar. 2003. The first PCA mode, explaining 74.8% of the variance of the nonlinearly projected Z500 anomalies, gives a typical PNA pattern (Fig. 2b) with main variability over the North Pacific and North America. This pattern displays the linear component of the Z500 signal associated with the SST index, as the first PC (solid curve in Fig. 2a) is correlated at above 0.99 with the SST index. The second PCA mode, explaining 25.2% of the variance of the nonlinearly projected Z500 anomalies, reveals a spatial pattern (Fig. 2c) resembling the one shown in Fig. 1c or 1f. The second PC (dashed curve in Fig. 2a) has positive values not only during the El Niño years (1958, 1966, 1973, 1983, 1992 and 1998), but also during La Niña years (1950, 1956, 1971, 1974, 1976, 1989, 1999 and 2000). Reversing the sign of the solid curve (PC1) when it is below zero yields a fair approximation to the dashed curve (PC2)— i.e. PC2 is noticeably positive whenever PC1 assumes large positive or negative values. Hence, regardless of warm or cold episodes, the Z500 has the same response pattern as depicted by Fig. 2c. This nonlinear component of the Z500 response to ENSO has about one third the variance of the linear component; furthermore, this nonlinear component (Fig. 2c) spreads the ENSO effect well beyond the North Pacific–North America domain of the linear component (Fig. 2b).

To further illuminate the nonlinear response, we consider a polynomial fit of the SST index to the Z500 anomaly at each grid point. Let T be the SST index, and $x_n = T^n$, then z, the Z500 anomaly (reconstructed from the 10 leading PCs) at a grid point, was fitted by $z = a_0 + a_1\hat{x}_1 + a_2\hat{x}_2 + \cdots + a_N\hat{x}_N$, where $\hat{x}_n$ is x_n normalized. For 400 bootstrap samples and for each spatial point of the Z500 anomaly field, regression coefficients $a_0, \cdots, a_N$ were computed. After ensemble-averaging over all bootstrap samples, a_n provided the spatial pattern associated with the nth order response to the SST index. When tested over independent data (i.e., data not selected in a bootstrap sample), the smallest MSE (averaged over all bootstrap samples) was found when $N = 2$, indicating overfitted results when $N > 2$. With $N = 2$, the ensemble-averaged values of a_1 and a_2 are plotted in Fig. 3.

The linear term (Fig. 3a) resembles the first PCA spatial mode of the nonlinear projection (Fig. 2b), confirming that this mode has captured the linear response of Z500 to ENSO. The quadratic term (Fig. 3b) resembles the second PCA mode of the nonlinear projection (Fig. 2c), as well as Figs. 1c and 1f, indicating that the nonlinear response of the Z500 anomalies to ENSO is mainly a quadratic response. As adding cubic terms and beyond to the polynomial fit leads to overfitting, higher order nonlinear response could not be detected robustly.

4 Summary and discussion

A fully nonlinear projection of the ENSO SST index to the Northern Hemisphere winter (November to March) Z500 monthly anomalies has been achieved using neural networks. During extreme warm and cold episodes, asymmetric Z500 patterns occurred not only over North America but also over the Euro-Atlantic region. The Z500 anomalies from the NN projection consist of a linear part, which resembles the traditional PNA pattern with anomalies largely confined over North Pacific and North America, and a nonlinear part, which reveals positive Z500 anomalies over the central-eastern North America, North Atlantic and western Europe, and negative Z500 anomalies over the west coast of North America, Scandinavia and eastern Europe regardless of the sign of the SSTA. The nonlinear component (with about 1/3 as much variance as the linear component) excites the positive PNA and positive NAO patterns. A polynomial study further indicates this nonlinear component to be a quadratic response to the SSTA.

In Fig. 2b, c or Fig. 3a, b, over the Euro-Atlantic region, the nonlinear part of the Z500 anomalies is much stronger than the linear part, indicating that the Euro-Atlantic winter climate mainly responds to ENSO nonlinearly. Thus an implication of this work is that to statistically predict the North Hemisphere, especially the European, winter climate from the tropical Pacific SST anomalies, a nonlinear forecast model is needed.

Acknowledgements

The authors acknowledge the support from the Natural Sciences and Engineering Research Council of Canada via research and strategic grants.

References

Deser, C., and M.L. Blackmon, On the relationship between tropical and North Pacific sea surface temperature variations, *J. Clim.*, **8**, 1677-1680, 1995.

Efron, B., and R.J. Tibshirani, *An Introduction to the Bootstrap*, CRC, Boca Raton, 1993.

Hannachi, A., Toward a nonlinear identification of the atmospheric response to ENSO, *J. Clim.*, **14**, 2138-2149, 2001.

Hoerling, M.P., A. Kumar, and M. Zhong, El Niño, La Niña and the nonlinearity of their teleconnections, *J. Clim.*, **10**, 1769-1786, 1997.

Hoerling, M.P., A. Kumar, and T. Xu, Robustness of the nonlinear climate response to ENSO's extreme phases, *J. Clim.*, **14**, 1277-1293, 2001.

Hsieh, W.W., and B. Tang, Applying neural network models to prediction and data analysis in meteorology and oceanography, *Bull. Am. Meteorol. Soc.*, **79**, 1855-1870, 1998.

Hsieh, W.W., Nonlinear canonical correlation analysis of the tropical Pacific climate variability using a neural network approach, *J. Clim.*, **14**, 2528-2539, 2001.

Hurrel, J.W., Decadal trends in the North Atlantic Oscillation: regional temperatures and precipitation networks, *Sciences*, **269**, 676-679, 1995.

Kalnay, E., M. Kanamitsu, R. Kisler, W. Collins, D. Deaven, L. Gandin, M. Iredell, S. Sasha, G. White, J. Woolen, Y. Zhu, M. Chelliah, W. Ebisuzaki, W. Higgins, J. Janowiak, K.C. Mo, C. Ropelewski, J. Wang, A. Leetmaa, R. Reynolds, R. Jenne, and Dennis Joseph, the NCEP/NCAR 40-year reanalysis project. *Bull. Am. Meteorol. Soc.*, **77**, 437-471, 1996.

Montroy, D.L., M.B. Richman, and P.J. Lamb, Observed nonlinearities of monthly teleconnections between tropical Pacific sea surface temperature anomalies and central and eastern North American precipitation, *J. Clim.*, **11**, 1812-1835, 1998.

Pozo-V*á*zquez, D., M.J. Esteban-Parra, F.S. Rodrigo, and Y. Castro-D*í*ez, The association between ENSO and winter atmospheric circulation and temperature in the North Atlantic region, *J. Clim.*, **14**, 3408-3420, 2001.

Sardeshmukh, P.D., G.P. Compo, and C. Penland, Changes of probability associated with El Niño, *J. Clim.*, **13**, 4268-4286, 2000.

Shabbar, A., B. Bonsal and M. Khandekar, Canadian precipitation patterns associated with Southern Oscillation, *J. Clim.*, **10**, 3016-3027, 1997.

Wallace, J.M., and D. Gutzler, Teleconnection in the geopotential height field during the Northern Hemisphere winter. *Mon. Wea. Rev.*, **109**, 784-812, 1981.

Wu, A., W.W. Hsieh, and F.W. Zwiers, Nonlinear modes of North American winter climate variability derived from a general circulation model simulation, *J. Clim.*, **16**, 2325-2339, 2003.

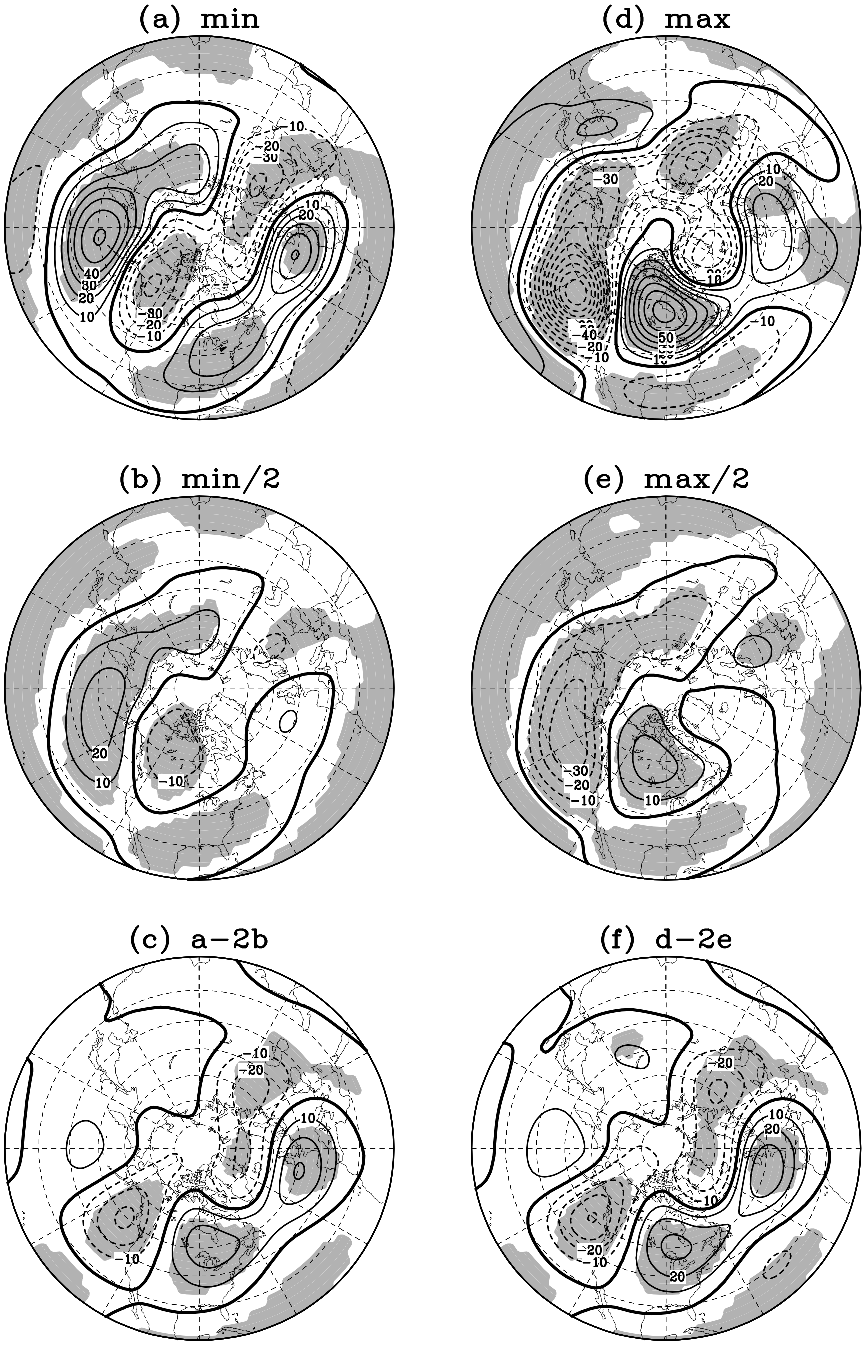

Figure 1: The Z500 anomalies associated with (a) the minimum SST index and (d) maximum SST index, and with (b) one half of the minimum SST and (e) one half of the maximum SST. The Z500 anomalies in panel (a) minus twice the anomalies in (b) are shown in panel (c); and the anomalies in panel (d) minus twice the anomalies in (e) are shown in panel (f). If the Z500 response to the SST index is strictly linear, then (c) and (f) will show zero everywhere. Contour interval is 10 meters and the grey areas indicate statistical significance at the 5% level, based on the distribution of the results from the 400 bootstrap samples.

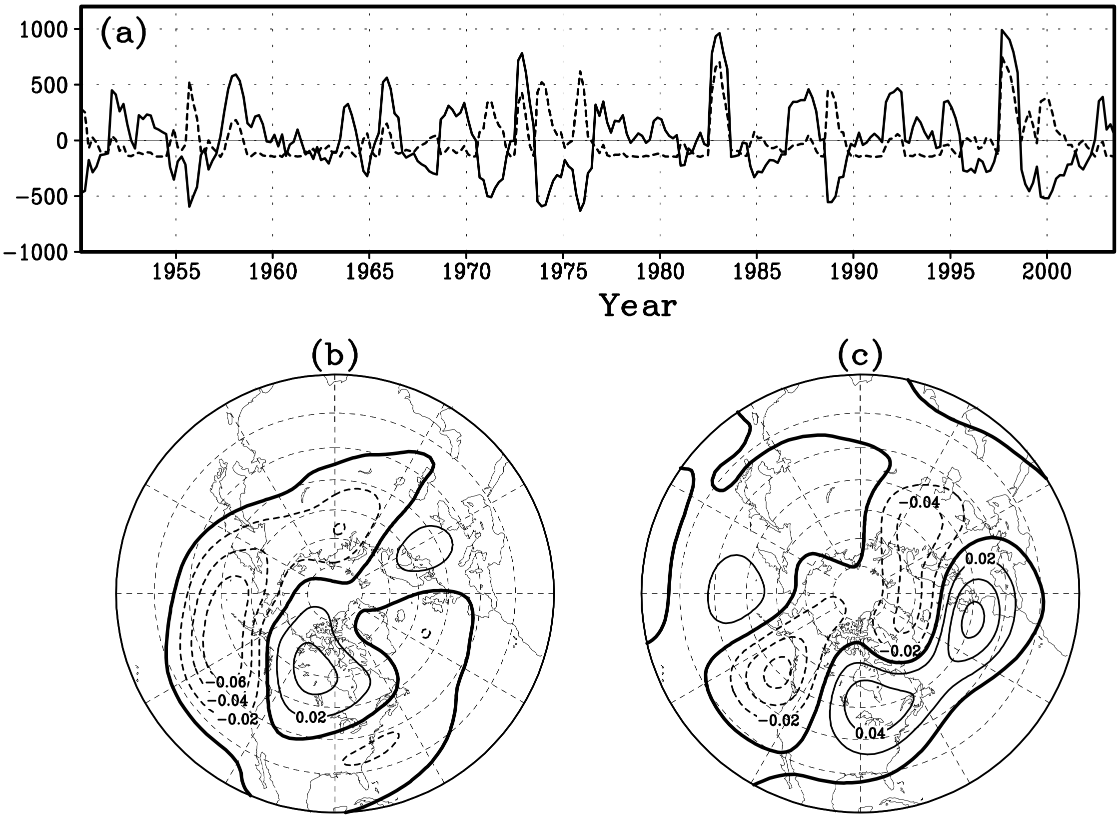

Figure 2: The 2 leading PCs of the Z500 anomalies associated with the ENSO SST index as extracted by the NN projection. The solid line in panel (a) represent the first mode, and the dashed line, the second mode. The corresponding 2 PCA spatial modes are shown in panels (b) and (c), respectively. The contour interval is 0.02, and the spatial modes have been normalized to unit norm.

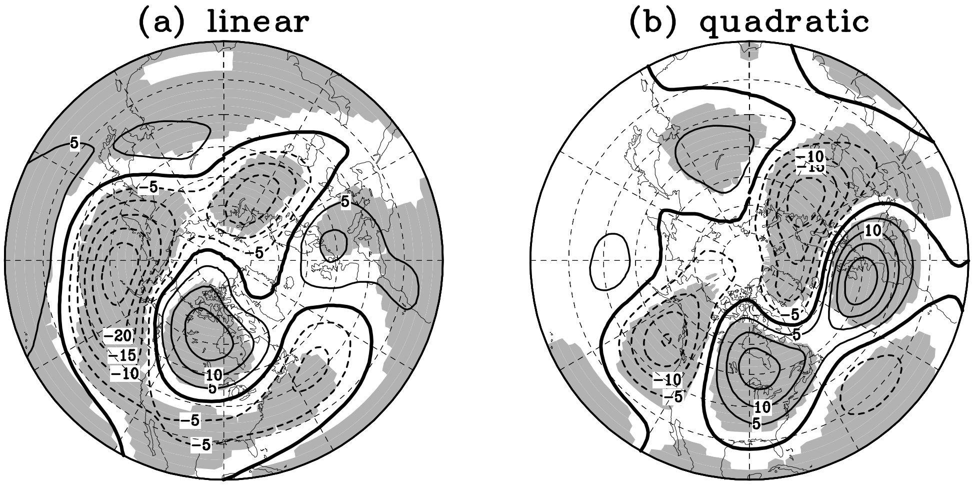

Figure 3: The Z500 anomaly patterns associated with the linear and quadratic terms of the tropical Pacific SST index. The contour interval is 5 meters and the shaded areas indicate statistical significance at the 5% level.